Taheri and Clark *Int J Concr Struct Mater* (2021) 15:8
https://doi.org/10.1186/s40069-020-00449-2

International Journal of Concrete Structures and Materials

RESEARCH Open Access

Preparation of Self-healing Additives for Concrete via Miniemulsion Polymerization: Formulation and Production Challenges

Shima Taheri[1*] and Simon Martin Clark[2]

Abstract

Concrete structures undergo internal damage; this usually starts at the atomic level with defects that then grow and form cracks, which can propagate through the material. Here, a method of preparation of poly(methyl methacrylate) (PMMA) nanocapsules adhesive system via miniemulsion polymerization technique is reported, where MMA + DMA (resin + accelerator) and BPO (hardener) components are separately encapsulated by PMMA shells. The crack-healing potential of these nanocapsules was then investigated by embedding them into the mortar matrix. The prepared PMMA core–shell self-healing nanostructures survived the mixing and hardening processes, and the hardened mortar alkaline environment. The stress fields associated with propagating cracks (load-induced cracking) broke the brittle/weak inert shell of these core–shell structures, resulted in releasing the healing agents to bridge the nascent and early-stage fractures (< 10 µm) in a short time. Long-term healing was achieved through the formation of polymorph calcite crystals in the presence of moisture and CO_2, which improved the durability of mortar by filling the gaps. Formulation design (addition of chemical admixtures) and process parameters (blade design and mixing speed) were found to directly impact the uniform distribution of nanocapsules, the survival rate of nanocapsules, and the overall strength of the hardened concrete. The stepwise approach to formulate and fabricate a novel high-strength self-healing concrete system unlocks unique opportunities to design nanomaterials that safeguard the integrity of concrete structures.

Keywords: self-healing concrete, miniemulsion polymerization, PMMA nanocapsules, concrete crack, crack healing

1 Introduction

Concrete is an essential building material used in the majority of structures. The demand for concrete-based infrastructures rises each year in line with population growth. (ABS 2018; BCI_Economic 2018) Concrete structures undergo internal and external damages; degradation of concrete over time increases the life-cycle cost of an asset by an estimated annual cost of billions of dollars to national economies.(Pacheco-Torgal et al. 2017) One problem among many that can endanger the durability and the reliability of concrete structures is cracking (Danish et al. 2020; Taheri 2019; Frosch and Jeffrey 2007); this usually starts at the atomic level with defects that then grow and form cracks which can propagate through a structure and can lead to more serious problems such as accelerated penetration of aggressive agents and subsequent corrosion of embedded reinforcing steel, weakening of the structure, and spalling of concrete cover. Furthermore, the majority of cracks occur deep within the concrete in inaccessible areas that are invisible to normal inspection, causing a major serviceability problem. Controlling and stopping crack propagation and enlargement is thus key to protecting concrete structures, enhancing their performance and reliability, and prolonging their service life. Self-healing of cracked

*Correspondence: shimataheri@yahoo.com
[1] Faculty of Science and Engineering and Centre for Nanoscale BioPhotonics, Macquarie University, North Ryde, NSW 2109, Australia
Full list of author information is available at the end of the article
Journal information: ISSN 1976-0485 / eISSN 2234-1315

concrete, therefore, can be an answer for sustainable infrastructures, as it can inhibit the development of early age microcracks into larger cracks. Self-healing materials spontaneously heal damage without the need for detection by human or any type of manual intervention (Wool 2008).

Over the past few years, scientists have developed promising technologies for internal healing of concrete cracks using encapsulated spores of limestone-producing bacteria.(Van Tittelboom and Belie 2013; Souradeep and Kua 2016; Tziviloglou et al. 2016) Bacterial spores lie dormant until moisture penetrates through the crack lines, triggering the spores to germinate and produce limestone that eventually seals the crack. Although this green approach is quite appealing and plausible, bacteria self-healing is a low-speed approach (> days), ideal for surface-only fractures and structures located in areas with high levels of relative humidity or in direct contact with a lot of water, such as marine structures or sewer pipes. In addition, a deteriorated structure loses its strength and integrity as a result of crack formation, and these might not be repaired by limestone filler on its own.(Gupta et al. 2017; Tziviloglou et al. 2016) The chemical healing approach is thus more consistent and applicable. Adhesives such as epoxies, acrylates or a hybrid of the two are ideal for bonding most common construction materials such as metal and are popular in filling gaps and repairing cracks (especially dormant cracks) in concrete. Moreover, they can be formulated into fast curing systems with around a few minutes work-life (the time needed before an adhesive harden and dry). The adhesive builds up the strength shortly after curing and, when custom-designed, without the need for external elements such as moisture.

Over the past 40 years, methyl methacrylate (MMA) has found applications in concrete production including in the polymer–cement composites (Short, 2007; Yeon et al. 2018), and the self-healing concrete (Dry and Mcmillan 1996; Dry 2000; Van Tittelboom et al. 2011; Alghamri et al. 2016). One of the biggest challenges in the direct incorporation of the monomeric MMA in concrete formulation or the impregnation of cement/aggregate with MMA monomer, as self-healing agent, is the hydrolysis of MMA in highly alkaline environments, which produces methacrylic acid and methanol. During the cement hydration, the formed methacrylic acid reacts with calcium hydroxide and forms calcium methacrylate [$H_2C{=}C(CH_3)CC{=}OO)_2Ca$] which is highly water soluble and might leach from the cement paste (CP) (Short 2007). Another concern could be absorption of MMA monomer by the cementitious phase before mixing with the initiator as the density of the MMA monomer is lower than 1 [0.936 g/mL at 25 °C (lit.)]. Hence, to protect the MMA monomer from cement alkaline environment, for a long-term self-healing purpose, they are needed to be packaged (or coated) prior to incorporation in a cementitious matrix.

Micro- and nano-encapsulation have been shown to be a promising technique in preserving drugs and healing agents in the past. (Musyanovych and Landfester 2014; Taheri et al. 2014a; Zhao et al. 2012; Ahangaran et al. 2019) In the microencapsulated self-healing approach, the healing components and/or catalysts (as core substances) are enclosed within a brittle/weak inert coatings/shells (containers) which can be ruptured easily to release its component.(Van Tittelboom and Belie 2013; Zhao et al. 2012; Landfester 2009) The shell of the self-healing containers in concrete applications should have a moderate strength and capable of rupturing easily to release its components under crack-induced stresses; however, it should be robust enough to survive the concrete-mixing process, and the emplacement. The shell surface should also have a high interfacial bond strength with the surrounding matrix so that they are mechanically linked to the cement paste and other components of concrete. The core material can be in the form of solid, liquid or even gas, and the composition of the shell material varies from expanded clay to gelatin, wax, paraffin, PU, glass, ceramic, silica, and silica gel. The size of the microcapsules varies from nanoscale to microscale, a typical size range is 500 nm–7000 μm. Larger microcapsules have more healing agent per unit area and more healing properties.(Hassan et al. 2016). The shape can be spherical, cylindrical or irregular.(Landfester 2009; Talaiekhozan et al. 2014; Van Tittelboom and Belie 2013; De Belie et al. 2018; De Rooij et al. 2011; Gupta et al. 2017) It is possible to have a mixture of spherical and cylindrical microcapsules in a matrix, although spheres seem better able to survive the mixing process. White et al. (White et al. 2001) were the first to report a practical demonstration of self-healing materials through embedding encapsulated healing agents into a polymer matrix containing dispersed catalysts.

This study focuses on the development of two-part (2K) self-healing adhesive materials, based on poly(methyl methacrylate) (PMMA), for healing of small microcracks in cementitious products (e.g., mortar, concrete, etc.), as shown in Fig. 1. Methyl methacrylate (MMA) adhesives are 2-part structural acrylic adhesives that are made of a resin (Part A hereafter) and a hardener (Part B hereafter). Mixing the resin and the hardener prompts a chemical reaction between the two and transforms them from a liquid state into a solid state, thus, two parts need to be packaged and stored separately prior to final usage. Parts A and B can contain a combination of different components: **Part A** comes in a liquid form and may contain a combination of MMA monomer, stabilizer (to prevent premature polymerization such as hydroquinone), accelerator (N,N-dimethyl-p-toluidine (DMPT), and N,N-dimethylaniline (DMA)). **Part B** comes in a powder form and may contain

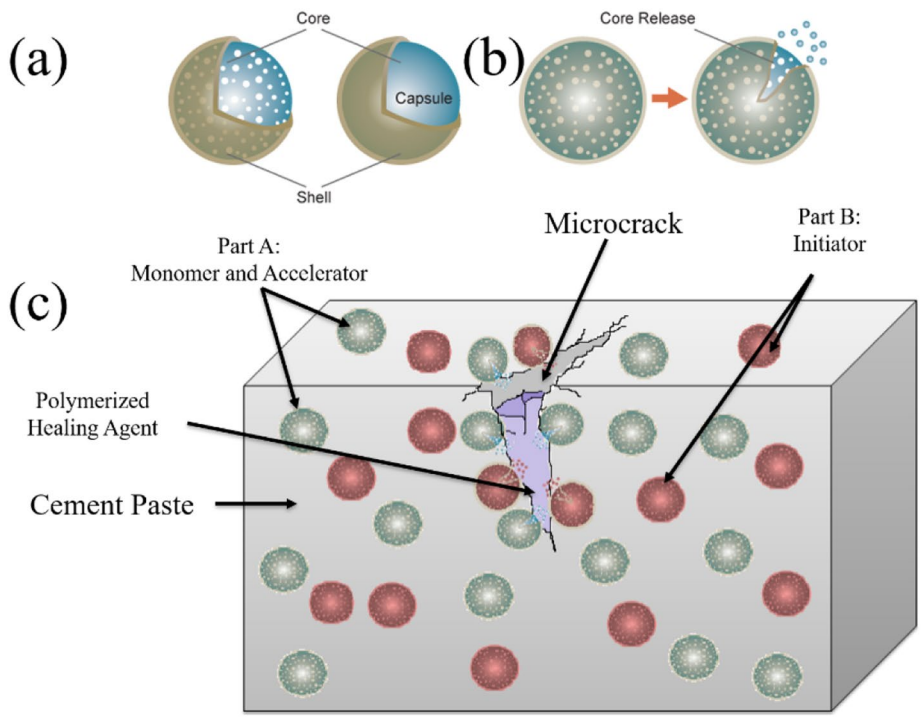

Fig. 1 Schematic representing nano- and microcapsule-based self-healing approach: **a** Nano/microcapsule core-shell structure, the core contains healing agent(s) or catalyst; **b** Triggered release of healing agent(s) by crack; **c** Crack healing mechanism, microcapsule shell is ruptured by damage and releases healing agent(s) to damage site. The reaction occurs upon contact of encapsulated healing agent A with B; the crack is then filled and healed.

a combination of pre-polymerized PMMA, PMMA, MMA copolymer beads and/or amorphous powder, radiopacifer (such as barium sulfate ($BaSO_4$), zirconia (ZrO_2)), and an initiator (BPO). Methyl methacrylate adhesive systems are ideal for applications where fast curing is required, or where lower application temperatures exist. High durability, elongated shelf life, crack-bridging capability, room temperature curing, and minimal bond shrinkage are among other key characteristics of these adhesives.(Dry and Mcmillan 1996; Van Tittelboom et al. 2011) Their versatility and ease of use make them the ideal choice for bonding a variety of substrates (Vaishya et al. 2013; Dry and Mcmillan 1996; Van Tittelboom et al. 2011) from artificial joints (bone–cement biomaterials), to metals, plastics, concrete, magnets, glasses, rubbers, and composites, and for interior and exterior applications in the biomedical, aerospace, automotive, construction, marine, composites, and transport fields.

A lot of research has been conducted on the encapsulation methodology (e.g., microencapsulation, extrusion) and the properties of the encapsulation materials (e.g., glass, polymeric) that can resist the mixing process of concrete. (Araújo et al. 2018; Hilloulin et al. 2015; Danish et al. 2020; Van Tittelboom and Belie 2013; Talaiekhozan et al. 2014) The application of glass is limited by the possibility of occurrence of the alkali–silica reaction; preparation of some capsules required lengthy time and heating; the need for surface treatment of capsules to trigger rupture for relatively small crack widths in concrete (~ 100 mm). The main objective of this study was to develop stable PMMA nanocapsules via the miniemulsion polymerization technique for self-healing of nascent and early-stage fractures (< 10 μm) in concrete. This method is attractive for the preparation of hybrid nanoparticles and nanocapsules. (Taheri et al. 2014a, b; Zhao et al. 2012) The miniemulsion polymerization technique offers far better control of the composition, particle size, and morphology compared to other encapsulation processes reported for the synthesize concrete self-healing additives (Landfester 2001; Beglarigale et al. 2018; Hassan et al. 2016). PMMA, as the shell material, has been shown to have a high chemical stability and good mechanical properties. PMMA is not affected by alkaline solutions and can resist in concrete alkaline environment. These unique properties, together with the biocompatibility of PMMA thermoplastics, make them suitable for a wide

range of applications, from biomedical to self-healing, textiles, and thermal energy storage. (Vaishya et al. 2013; Ahangaran et al. 2019; Khan et al. 2016; Sarı et al. 2014; Iqbal and Sun 2018; Zydowicz et al. 2002; Feuser et al. 2016).

In this study, three shell materials including potato starch, PLLA, and PMMA are examined. These materials can withstand the concrete alkaline environment and have the anticipated surface functional groups to improve the interfacial bond strength between the shell of capsules and concrete matrix. The nanocapsule properties, such as diameter, shell wall thickness, morphology, and surface functional groups, are characterized using scanning electron microscopy (SEM) and Fourier transform infrared spectroscopy (FTIR). Another objective of this study was to develop a production procedure for efficient incorporation of PMMA healing capsules in cementitious products such as concrete. A simple mortar formulation is used to demonstrate challenges in the incorporation of capsules in concrete, including retaining the functionality of capsules during mixing, a uniform distribution of capsules within the concrete matrix, and the impact of capsules on workability, and mechanical properties. The production procedure is refined by stepwise changes in the mixing parameters (mixing blade, and agitation rate), and the mix design (via the addition of dispersing agents, superplasticizers, shrinkage reducing agents, and copolymer binders). The microstructural and mechanical properties of developed self-healing mortar specimens are assessed using SEM, compressive strength, and three-point bending methods.

2 Experimental Section

2.1 Materials

All chemicals were used as received without further purification. Poly(methyl methacrylate) (PMMA, average Mw ~ 350,000), methyl methacrylate (MMA), benzoyl peroxide (BPO, Luperox® A98), N,N-dimethylaniline (DMA), N,N,4-trimethylaniline (DMPT), poly(L-lactic acid) (PLLA, average Mn 40,000), 2,4-toluene diisocyanate (TDI), water-soluble starch from potato, dichloromethane (DCM, CH_2Cl_2), cyclohexane (> 99.9%), chloroform ($CHCl_3$), sodium chloride (NaCl), polyvinyl alcohol (PVA), and nuclease-free sterilized water were purchased from Merck and Sigma-Aldrich, Australia. The oil-soluble surfactant polyglycerin-polyricinoleate (PGPR) was custom-made by Kemix, Australia. Sodium dodecyl sulfate LR (SDS) was purchased from Chemsupply Pty Ltd, Australia. The non-ionic surfactant Lutensol AT50, MasterGlenium® SKY 8100 and MasterLife® SRA 200 were kindly provided by BASF, Australia. DISPERBYK-191 and DISPERBYK-192 (D-191 and D-192) were kindly provided by ResChem Technologies, Australia. The binding material used in the preparation of mortar samples was Bastion General Purpose Cement, and according to Australian Standard AS3972, Type GP. ETONIS® LL5999-8331 admixture (vinyl acetate–ethylene copolymer) was kindly provided by Wacker Chemicals, Australia. The fine aggregate used was wet white sand from Building Materials, Australia. Milli-Q water (resistivity 18.2 Ω) was used for preparation of STS-B and STS-C samples (as described in 2.4 and 2.5) and normal tap water (pH 8.1) was used for preparing mortar specimens (as described in 2.6).

2.2 Characterization

Microstructural analysis was conducted by scanning electron microscope (SEM). Two SEMs were used for this study, a Zeiss EVO MA15 SEM–EDS and a Phenom XL desktop SEM. SEM imaging of microcapsule samples was performed by drying a droplet of a diluted sample on the silicon wafer. The microcapsule samples imaged by a Phenom XL desktop SEM were coated with a thin layer of gold using an Emitech K550 gold sputter coater, and samples imaged by a Zeiss EVO MA15 were carbon coated using a BOC Edwards AUTO 306 vacuum coater, to reduce space charge effect. Mortar samples were only imaged using the Phenom XL desktop SEM, they were used unpolished without any prior surface preparation to preserve crystalline structures. The size and distribution of particles were analyzed by ImageJ Software. (Schindelin et al. 2012) Thermo Scientific™ Nicolet™ iD5 Fourier transform infrared (FTIR) Spectrometer was used to determine the chemical composition of the self-healing microcapsules, in the spectral range between 4000 and 500 cm^{-1}. The three-point flexural test of prismatic specimens was measured using an Instron 5982 Universal Testing Machine, with a maximum 100-kN static compressive load and following ASTM C78/C78M-18. (ASTM 2018b) The compressive strength of mortar cylinders was tested using an Instron 8036 testing machine with a 10,000-kN static compressive load, following the ASTM C39/C39M-18 Standard (ASTM 2018a), with a loading rate of 0.25 ± 0.05 MPa/s. Analysis of samples were performed at ambient temperature and in triplicate.

2.3 Synthesis of Self-healing Additives

2.3.1 Potato Starch Self-healing Nanocapsules

Part A: To an aqueous solution consisting of 1.4 g sterilized water, 1.0 mg NaCl and 0.3 g soluble potato starch (water phase), a mixture of 10.0 g of cyclohexane premixed with 0.1 g PGPR, 1 g MMA, 0.3 g PMMA, and 40.0 mg DMPT (oil phase 1) was added and stirred at 1000 rpm for one hour at 25 °C using a magnetic stirrer. Then the mixture was ultrasonicated for 60 s at 50% amplitude in a pulse regime (10 s sonication, 10 s pause)

using a Branson SFX550 Sonifier and a 1/200 tip under ice cooling conditions in order to prevent evaporation of the solvent. Then oil phase 2 containing 0.3 g TDI dissolved in 5.0 g of cyclohexane and pre-mixed with 0.030 g PGPR was added dropwise over 5 min to the previously prepared emulsion under stirring conditions while maintaining the temperature at 25 °C. The mixture was kept under stirring overnight at 25 °C. The miniemulsion samples were then dispersed in 0.3% Lutensol AT50 at a ratio of 1:5. **Part B:** this part was prepared following the exact same procedure that was described for the Part A, except for the oil phase 1. This phase in Part B consists of a mixture of 10.0 g of cyclohexane pre-mixed *with* 0.1 g PGPR, 0.3 g PMMA, and 0.1 g BPO.

2.3.2 PLLA Self-healing Nanocapsules

Part A: 0.3 g PLLA pellets were dissolved gradually in 10 g $CHCl_3$ at 35 °C on a shaker for 60 min (oil phase). Then 0.2 g MMA, 0.1 g PMMA and 40.0 mg DMPT were added to this mixture and stirred at 1000 rpm for one hour at 25 °C using a magnetic stirrer. Two different water phase system studied: 0.15 g of SDS and 0.4 g of PVA were dissolved in 26 g Milli-Q water separately and then stirred for at least 30 min until dissolved. Then, the aqueous solution of surfactant (SDS or PVA) was mixed with the oil phase and mechanically stirred for 1 h at 1000 rpm at 25 °C to prepare the macroemulsion. Then the mixture was ultrasonicated for 120 s at 50% amplitude in a pulse regime (10 s sonication, 10 s pause) to prepare the miniemulsion using a Branson SFX550 Sonifier and a 1/200 tip under ice cooling conditions in order to prevent evaporation of the solvent. Next, the mixture was transferred into a round-bottom flask with a wide neck and stirred (400 rpm) in a water bath overnight at 40 °C to evaporate the chloroform. **Part B:** this part was prepared following the exact same procedure that was described for Part A, except for the oil phase. For Part B, the oil phase contained 0.3 g PLLA pellets dissolved in 10 g $CHCl_3$ and then mixed with 0.01 g BPO, and 0.1 g PMMA.

2.3.3 Self-healing Nanocapsules

Part A: 2.5 g PMMA was dissolved in 25.0 g DCM at 25 °C and then 2.5 g MMA, 0.3 g DMA were added to this mixture and stirred at 1000 rpm for one hour at 25 °C using a magnetic stirrer. Then, 25 g of the aqueous solution of 1% PVA was mixed with the oil phase and mechanically stirred for 1 h at 1000 rpm at 25 °C to prepare the macroemulsion. Then the mixture was ultrasonicated for 30 s at 50% amplitude in a pulse regime (5 s sonication, 10 s pause) to prepare the miniemulsion using a Branson SFX550 sonifier and a 1/200 tip under ice cooling conditions in order to prevent evaporation of the solvent. Next, the DCM was removed from the miniemulsion by rotary-evaporation overnight at 40 °C in a water bath. **Part B:** this part was prepared following the exact same procedure that was described for Part A, except for the oil phase. For Part B, the oil phase contained 2.5 g PMMA, 25.0 g DCM, and 0.5 g BPO.

2.4 Preparation of Self-healing Mortars

A typical mortar formulation consisting of 30% cement, 70% sand, and the water to cement ratio (w/c) of 0.43 was used as the guideline formulation for the preparation of control mortar and self-healing mortar samples, as summarized in Table 1. Powders were dry mixed in the mixing bowl. Part A and Part B were prepared in two separate containers using this procedure: first the amount of ingredients indicated by a star in Table 1 were divided in half and each half was mixed separately in two different containers. Then Part A was added to one container and Part B to the other container and they were mixed for 3 min at 1000 rpm using a magnet stirrer at RT. Then the aqueous solutions of Part A and Part B were added gradually into the mixing bowl while mixing at a low speed (200 rpm) using a paddle mixer and mixed for another 3 min until the right consistency was

Table 1 Mix proportions (in parts by weight) for the preparation of the self-healing mortar samples. Note: Part A (resin + accelerator) and Part B (hardener) prepared as described in Section 2.3.

Ingredient		F1 (ctrl)	F2	F3	F4	F5
Cement	Powder phase	30.00	28.90	28.85	28.85	28.55
Sand		70.00	69.77	69.63	69.63	68.91
LL5999-8331		–	–	–	–	0.98
Water*	Water phase	13.00	11.60	11.60	11.40	11.40
Part A		–	1.00	0.99	0.99	0.98
Part B		–	0.33	0.33	0.33	0.32
SKY 8100*		–	–	–	0.10	0.10
SRA 200*		–	–	–	0.10	0.10
BYK-191*		–	–	0.10	–	0.02
BYK-192*		–	–	0.10	–	0.02

achieved. Casting of specimens into molds (cubic, prism and cylinder) was started immediately upon completion of mixing. A shaker was used to remove air bubbles trapped in the cement mixture. Specimens were demolded 24 h after casting and then immersed in a water bath for the duration of 28 days.

3 Results and Discussion

3.1 Synthesis and Characterization of Self-healing Capsules

Self-healing micro- and nano-capsules were synthesized via the miniemulsion polymerization technique, as described in the Sect. 2 in this paper and summarized in Table 2, based on methods previously published by the author. (Taheri et al. 2014a, b).

The SEM micrographs of synthesized Part A micro- and nano-capsules are shown in Fig. 2. An inverse (water-in-oil) miniemulsion technique was applied to prepare STS-A (Fig. 2a). In this method, the capsule shell was formed by cross-linking of the starch -OH groups with the NCO groups of TDI (crosslinker). These capsules were expected to re-disperse as individual capsules once they were transferred from the cyclohexane to an aqueous medium containing the non-ionic surfactant (i.e., Lutensol AT50) (Taheri et al. 2014a).

Contrary to what was expected, these nanocapsules linked to adjacent nanocapsules from the surface (Fig. 2a), indicating that the release of the free radicals during the cross-linking step initiated the polymerization of MMA monomers at the surface of these capsules.

Table 2 Summary of the formulations and the techniques used in the synthesis of self-healing micro- and nano-capsules.

Sample ID	Shell material	Synthetic technique	Part A		Part B	
			Oil phase	Water phase	Oil phase	Water phase
STS-A	Potato starch	Miniemulsion/polyaddition	1: cyclohexane PGPR MMA PMMA DMPT 2: cyclohexane PGPR TDI	Sterilized Water Potato Starch NaCl	1: cyclohexane PGPR PBO PMMA 2: cyclohexane PGPR TDI	Sterilized Water Potato Starch NaCl
STS-B	PLLA	Miniemulsion/solvent evaporation	Chloroform PLLA MMA PMMA DMPT	SDS/PVA Milli-Q Water	Chloroform PLLA BPO	SDS/PVA Milli-Q Water
STS-C	PMMA	Miniemulsion/solvent evaporation	DCM MMA PMMA DMA	PVA Milli-Q Water	DCM PMMA BPO	PVA Milli-Q Water

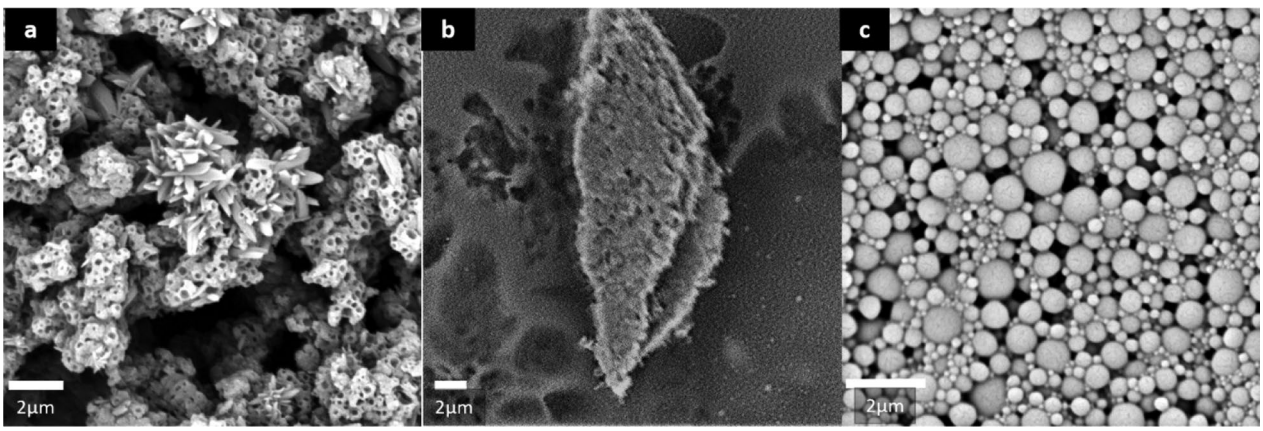

Fig. 2 SEM micrographs of Part A nanocapsules prepared from different shell materials and encapsulation techniques. **a** STS-A: the potato starch capsules synthesized via the miniemulsion/polyaddition polymerization process. **b** STS-B: the PLLA capsules synthesized via the miniemulsion/solvent evaporation process; **c** STS-C: the PMMA capsules synthesized via the miniemulsion/solvent evaporation process.

Although STS-A capsules are much smaller in size (compared to STS-B and STS-C), they are agglomerated and thus were not suitable for our intended application. In STS-B (Fig. 2b), PLLA was used to package the self-healing components. Again, the SEM revealed that these nanocapsules, despite having spherical shapes, were agglomerated and glued together. The only successful procedure, according to the SEM micrographs (Fig. 2c), was the encapsulation of self-healing agents using poly(methyl methacrylate) (PMMA) or STS-C nanocapsules. A more detailed presentation of this method is presented in Fig. 3a. For Part A (Fig. 3b), a combination of MMA (monomer) and DMA (accelerator) was encapsulated, and for Part B (Fig. 3b) only BPO (initiator) was encapsulated. After mixing the monomer, the initiator and the accelerator through free radical polymerization, the adhesive hardened into a solid material (Fig. 3c).

The surface chemistry of STS-C nanocapsules was then characterized using FTIR spectroscopy. FTIR spectra of

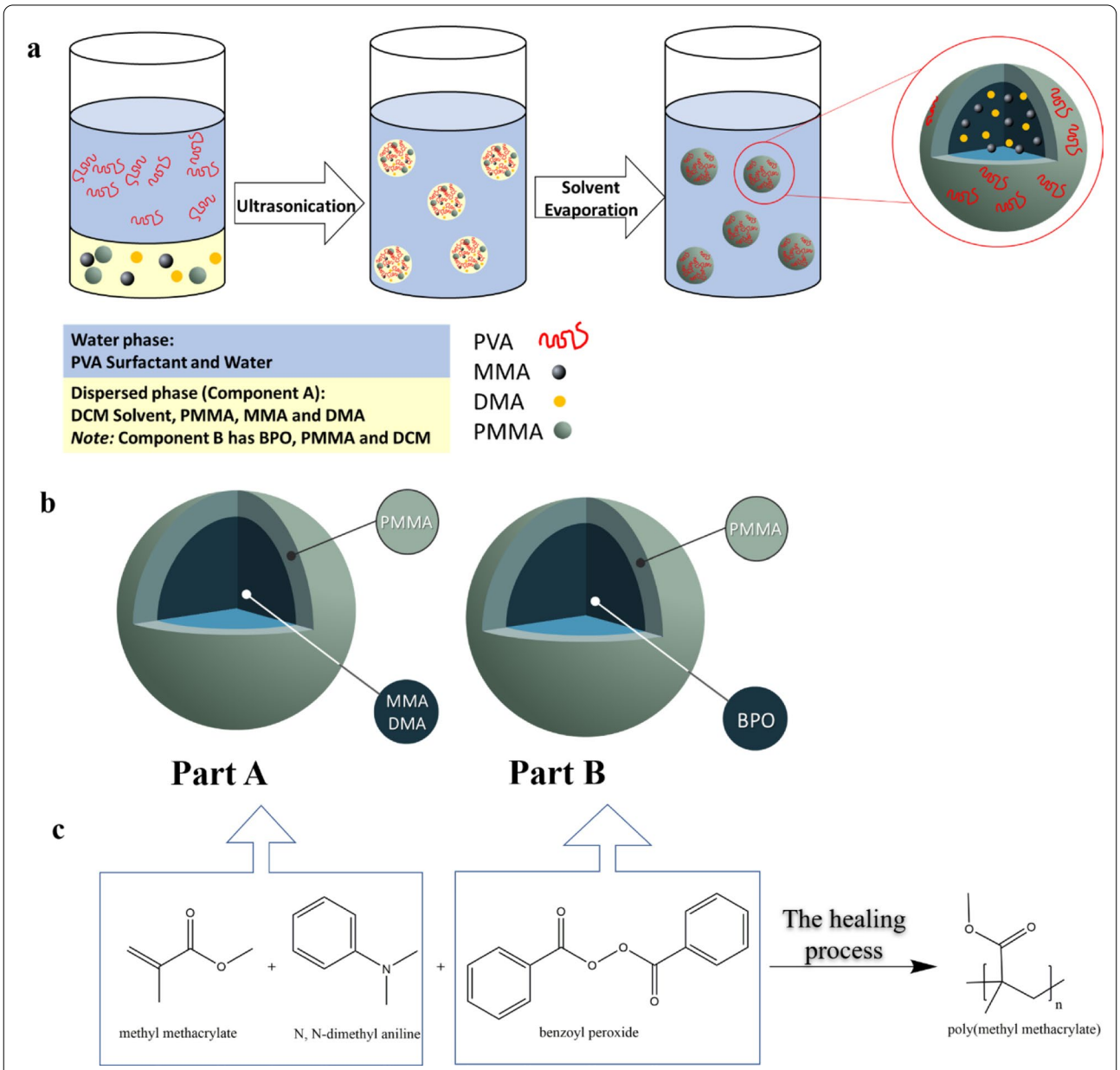

Fig. 3 **a** Formation of the PMMA-based self-healing additives using the miniemulsion/solvent evaporation technique. **b** Schematic of the 2K hybrid PMMA self-healing core–shell structures. **c** Activation of the healing process upon cracking and capsules break.

these hybrid nanostructures (Fig. 4) are dominated by the peaks corresponding to PMMA polymer (see inset in Fig. 4) (Tommasini et al. 2018). The band around 1750 cm^{-1} is due to the stretching of carbonyl groups (C=O), belonging to the PMMA polymer. The band 995 cm^{-1} is due to RHC=CH_2. The band at 3366 cm^{-1} appears to be an overtone band having frequency twice that of C–O stretching frequency. A band at 1224 cm^{-1} is due to C–O–C stretching. PMMA characteristic bands observed at 3020–2950 cm^{-1} are $-CH_3$ and CH_2 stretching, respectively. The corresponding bending peak occurs at 1449 cm^{-1}.

STS-C nanocapsules' morphology was further analyzed using the low-vacuum mode of a benchtop SEM as well as a high vacuum SEM–EDS (as shown in the insets of Fig. 5a, b). Due to the drying and the vacuum required for SEM–EDS imaging, the nanocapsules appear in the insets like hollow half balls (already ruptured). Analysis of SEM images by ImageJ software showed that Part A particles (Fig. 5a) were poly-disperse structures and had an average size distribution of 400 ± 100 nm, a maximum particle size of 1400 nm, and an average shell thickness of 50 ± 5 nm. Part B particles (Fig. 5b) were poly-disperse structures and had a size distribution of 900 ± 100 nm on average, a maximum particle size of 2000 nm and an average shell thickness of 60 ± 10 nm. As stated earlier, shell thickness plays an important role in preserving the content until the final setting of concrete. The size of the Part A and Part B nanostructures was controlled by the duration of ultrasonication and the intensity used (Taheri et al. 2014a; Landfester, 2001). To have bigger capsules, macroemulsions were sonicated for only 30 s at 50% amplitude in a pulse regime (5 s sonication, 10 s pause). Ultrasonication generates excessive heat, so the nanocapsules were synthesized under ice-cold condition and the system was pulsed on/off s to reduce this effect. Longer ultrasonication times resulted in particles smaller than 500 nm, which made them very difficult to distinguish from other components and crystals present in a cement paste during SEM analysis. The duration of the ultrasonication and the initial amount of PMMA (as the shell material) had a linear correlation with the shell wall thickness (data not shown).

Part A and Part B were blended in a ratio of 1:0.3 at 23 °C and laboratory relative humidity of ~ 70%. The mixture was immediately placed on a silicon wafer and dried, then it was imaged using an SEM (Fig. 5c). No excess force was used to mix the two parts. Thus, the distribution of Parts A and B (in this particular experiment) is not uniform. It can be seen that the shell of one of the Part B capsules (identified by their bigger size) had already fractured, and the reaction between the two components started. A centrifuge was then used to mix Part A and Part B (in the ratio of 1:0.3 and 1 min at 10,000 rpm) in order to assess their reactivity. After removing the supernatant, a sample from the very viscose material precipitated at the bottom of the vial was placed on a silicon wafer, dried and imaged by SEM (Fig. 5d). The rotation forces were high enough to break the capsules and a uniform polymer film formed as a result of the reaction between Part A and Part B. No unreacted particle could be detected in this sample.

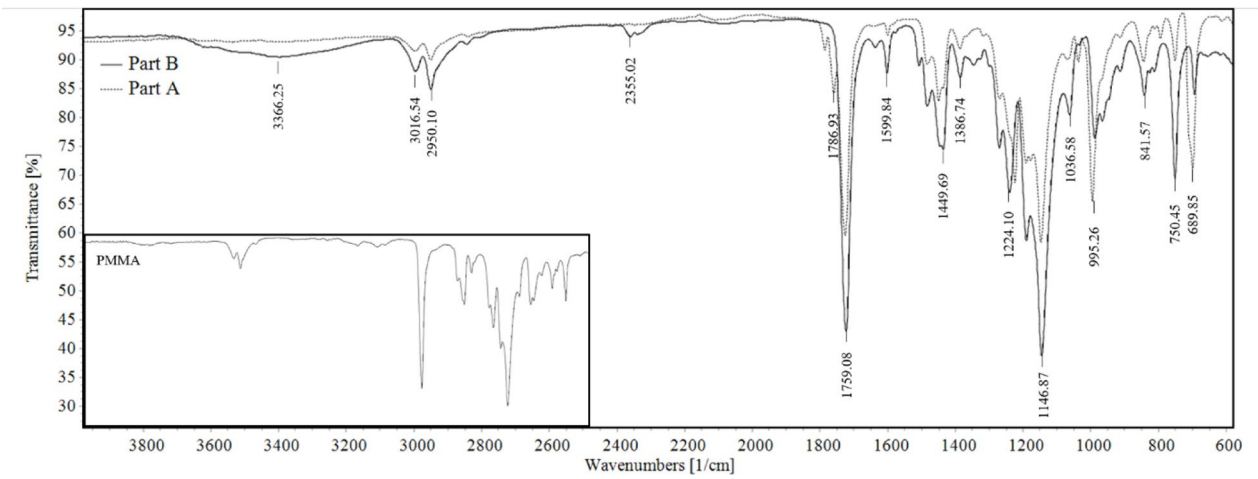

Fig. 4 FTIR spectra of the STS-C self-healing nanocapsules Part A and Part B. The inset is the FTIR spectra of PMMA-only core–shell structures without any core material (used as control).

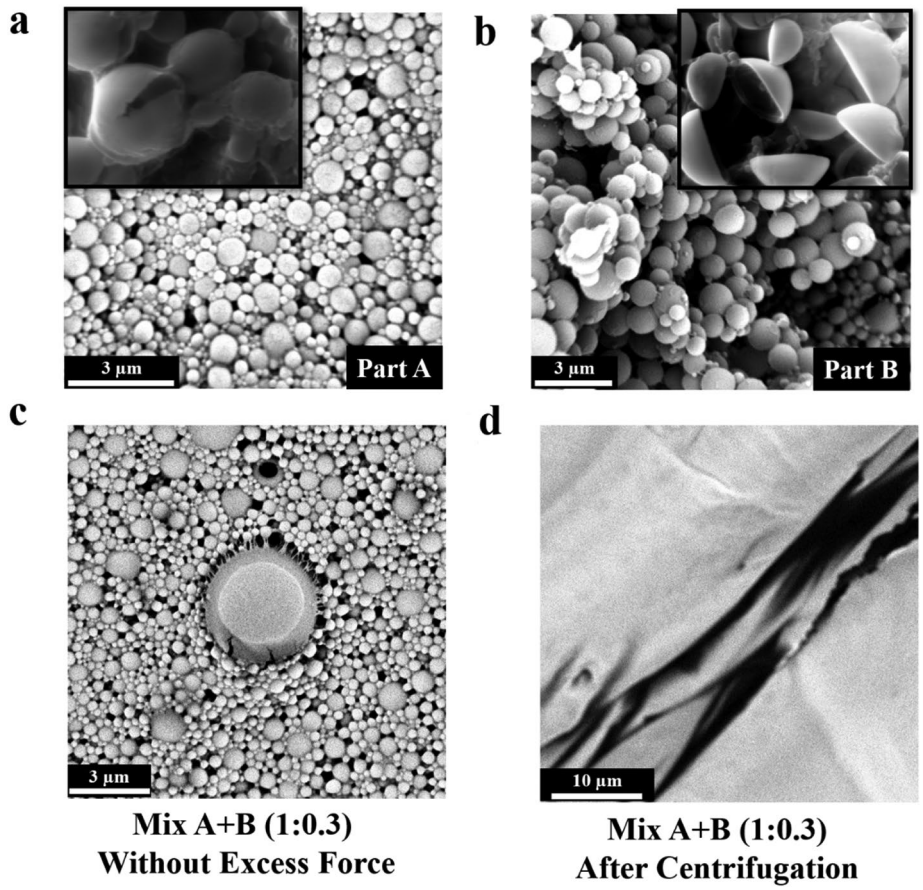

Fig. 5 SEM micrographs of Part A (**a**), and Part B (**b**). The insets are higher magnification SEM–EDS imaging. The SEM of freshly mixed Part A and B in the ratio of 1:0.3 without using excess force (**c**), and the SEM of the mix of Part A and B in the ratio of 1:0.3 after centrifugation.

3.2 Preparation of Self-healing Mortar and Characterization

The ultimate aim of this study was to develop a production procedure for efficient incorporation of PMMA healing capsules in concrete products. Further objectives were to avoid capsule breakage during concrete mixing, to obtain uniformly dispersed capsules within the matrix, and to make this system practically applicable at the commercial level. Previous studies have shown that the performance of the concrete can be estimated from the results obtained in the corresponding mortars (Camões et al. 2005; Rubio-Hernández et al. 2012). Therefore, we used mortar mixes for the incorporation of encapsulated healing agents (Part A and Part B). Control mortar samples (without self-healing additives) were prepared using the F1 formulation (Table 1). F1 was also used as the starting formulation to design the self-healing concrete systems (F2 to F5). SEM technique was employed to assess the survival and distribution of nanocapsules as well as the effectiveness of mixing procedures. During this study, no surface polishing was applied to the sample used for SEM analysis in order to preserve the crystalline structures and morphologies of sample surfaces. The stepwise approached used to optimize the concrete-mixing strategy and the mix design will be explained in the following paragraphs.

Initially, the F2 formulation (Table 1) was employed to investigate the crack-healing potential of STS-C self-healing additives. Once the F2 mortars were hardened (after the standard 28Ds hardening procedure), they were cut in half using an IsoMet™ Low Speed Saw, in order to study the distribution of Part A and Part B. Figure 6a is an SEM image of the surface of the one half of a mortar sample. Some of the capsules in this particular area were destroyed, either during the mixing or the cutting by the saw, resulting in the release and reaction of the encapsulated agents. Consistent with previous studies, one of the biggest challenges in the incorporation of encapsulated healing agents is survival of the mixing process. (Van Tittelboom and Bilie 2013) The distribution of Part A and

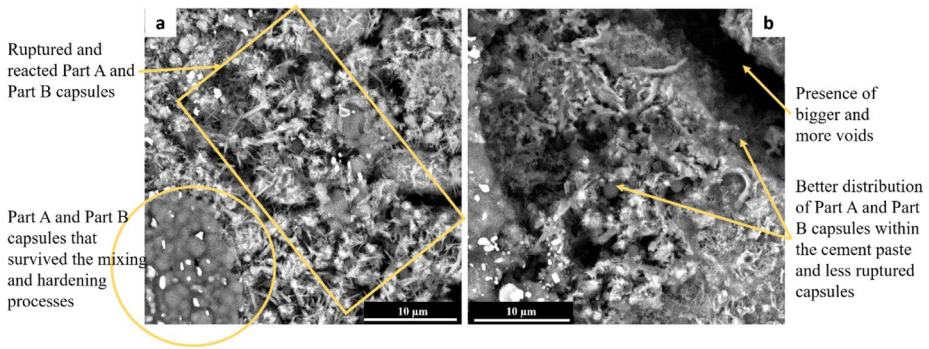

Fig. 6 Microstructure and morphology of the surface of self-healing mortar prepared using F2 (**a**) and F3 (**b**) (images taken after initial trials and prior to system optimization).

Part B was also found to be unsatisfactory. Some areas, highlighted in Fig. 6a, had a large number of capsules, while no capsules could be detected in other areas, meaning that the presence of surface-attached PVA (Fig. 3a) could not guarantee the uniformity of capsule distribution in the cement paste matrix.

To solve the homogeneity issue, the effect of adding an external dispersing agent to the mortar formulation was then explored. Unfortunately, there is no commercially available dispersing agent in the market for this specific purpose. Therefore, the use of a few different wetting and dispersing additives—originally designed for aqueous coating systems, adhesives, and emulsion systems—was explored to check if they could be repurposed for this application. A combination of D-191 and D-192 in equal proportions was found to help with a better distribution of Part A and Part B through the cement paste (Fig. 6b). The mortar prepared using the F3 formulation (Table 1) was lightweight (compared to F1), and the shrinkage of dried samples was noted. This mortar was also highly porous (Fig. 6b).

The mixer configuration including mixing blade design was another important factor that improved the homogeneity of the Part A and Part B distribution. Two different mixing blades, an anchor blade and a ribbon blade, were studied, as shown in Fig. 7a. After trial and error, it was found that to achieve a uniform distribution of Part A and Part B, a ribbon blade and a mixing speed of < 200 rpm was required. The selection of the appropriate mixing blade together with optimization of the mixing speed directly affected both the uniformity of distribution of Part A and Part B microcapsules in the mortar sample and the capsule survival rate during the mixing process.

The optimization of the mortar formulation through the addition of commercially available concrete admixtures was then explored, to evaluate their effectiveness on reducing the number of voids, improving the workability, reducing the water intake, and improving the uniform

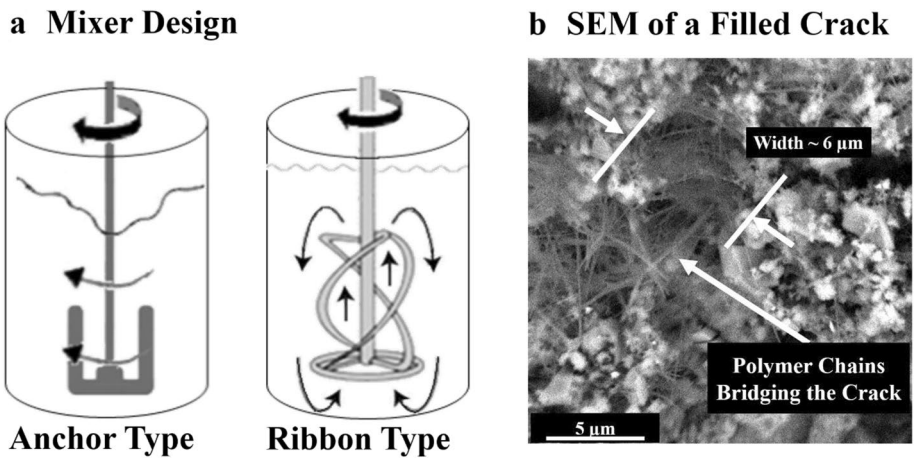

Fig. 7 **a** Concrete mixer design using an anchor-type blade and a ribbon-type blade; **b** SEM micrograph of a filled crack with healing products of Part A and Part B in a mortar prepared using F4.

distribution of Part A and Part B across the product matrix. Different combinations of MasterGlenium SKY 8100 (a second-generation polycarboxylic ether polymer superplasticizer), MasterLife SRA 200 (shrinkage reducing agent Type SN according to AS 1478), and ETONIS® LL5999-8331 (vinyl acetate–ethylene copolymer binder for enhancing adhesion properties and reducing voids) in self-healing mortar mixes were investigated and the F4 and F5 formulations were ultimately selected (Table 1). Parameters such as w/c ratio, mixing property, workability, dry-shrinkage property, and the casting of these formulations were all found to be superior to other formulations, in particular to F2 and F3 formulations. In addition, Part A and Part B were distributed evenly across the samples. The SEM image of the healing products and PMMA chains, that bridged a crack width of 6 µm, in the fractured sample of F4, is shown in Fig. 7b.

To examine the effect of the 2K PMMA-based self-healing additives on the mechanical properties of the concrete, the compressive strength of samples and the relationship between applied load versus displacement were studied (Fig. 8). The mixing process used for F2 samples was optimized to achieve the best possible distribution of Part A and Part B in the absence of dispersing agents and external admixtures.

As can be seen in the compressive strength graph, Fig. 8a, the incorporation of the self-healing components (F2) slightly (~4%) decreased the strength of the mortar (F1). This was possibly due to the replacement of 1% cement with the self-healing additive, or the non-uniform distribution of Part A and Part B across the matrix. In F3, while the addition of the dispersing agents assisted in the homogeneous arrangement of Part A and Part B across the cement matrix, it resulted in a significant reduction (~50%) in the compressive strength of the mortar. This was possibly due to the presence of excess voids (detected by SEM imaging, see Fig. 6b) or the weakening of the mortar structure due to the negative impact of adding a possibly unsuitable dispersing agent (even though it was found to be the best possible choice among other dispersing agents tested). In the absence of a dispersing agent, and through the addition of a superplasticizer and an anti-shrinking agent (in F4), the compressive strength of mortar formulations was enhanced by 60%. The F5 compressive strength results show that the addition of a binder could rectify the loss in compressive strength when dispersing agents were presented; nevertheless, the compressive strength was still 9% lower than the control formulation (F1). Previous studies have indicated that the primary considerations when designing a high-strength concrete are the size of the aggregate, the packing of the aggregate, the strength of the mortar, and the fineness of the admixtures, with the strength of the aggregate being only a secondary consideration. (De Larrard and Belloc 1997) In F4 formulation, a good selection of materials, a careful formulation, and the optimization of the production process resulted in a high-strength mortar, even in the absence of the coarse aggregates.

The load–displacement curves corresponding to the plain (ctrl) and self-healing mortars, obtained by the three-point bending test, are depicted in Fig. 8b. The F2, F4, and F5 self-healing mortars resist evolving nanoscale cracks, however, they show a sudden loss of load-bearing capacity after reaching the maximum load. This is possibly due to an insufficient amount of self-healing agents at the point of microscale cracks formation or fragility of the adhesive polymer bond. The F4 had the highest load-bearing capacity. The elastic-linear pre-cracking stage of

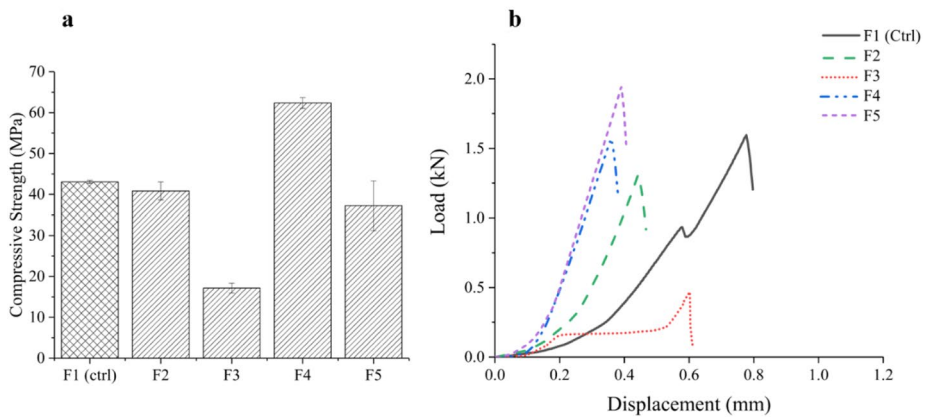

Fig. 8 **a** Compressive strength of 28D hardened control (F1) and self-healing (F2-F5) mortars samples. Each error bar represents the standard deviation of three measurements; **b** load–displacement curves of the control (F1) and the self-healing (F2-F5) mortars as measured by the three-point bend test.

F3 was much shorter and the first crack appeared at a load of 0.15 kN and a displacement of 0.2 mm. However, F3 demonstrated strain-softening behavior in contrast to the other specimens.

Once the samples were broken, the fractured surface morphology was studied using SEM (Fig. 9 and first row). The formation of needle-shaped adhesive bonds, as a result of the reaction between Part A and Part B, was apparent all over the surfaces of self-healing mortars. The length of these bonds, as estimated by the ImageJ software, was between 1 to 10 μm and the thickness was between 10–60 nm. Thus, a crack less than 10 μm width is expected to recover with this self-healing additive in a short time. These needles cannot be attributed to ettringite ($Ca_6Al_2(SO_4)_3(OH)_{12}{\cdot}26H_2O$) or aragonite ($CaCO_3$) crystals, since they were observed only in areas with ruptured nanocapsules (Figs. 6a and 9 first row) and this morphology cannot be detected on the surface of control (F1) mortars. In the self-healing mortars that did not experience a continuous load/cracking, these needle-shaped structures did not exist.

The cracked mortar samples used for the three-point bending test were then immersed in tap water (pH 8.1) for 7 days. SEM images (the second row of Fig. 9) show that the growth of calcite ($CaCO_3$) polymorph crystals (mainly in the form of octagonal and scalenohedral crystals) was accelerated in the self-healing mortars (F2-F5). The newly formed crystals were able to fill in most of the voids presented in the mortar samples prior to submerge in water. Calcite forms through the reaction between Ca^{2+} in concrete and CO_3^{2-} dissolved in water. It was shown that the carboxylate groups could control the calcite growth (Choi et al. 2017; Falini et al. 2007); therefore, the calcite formation was facilitated in the presence of polymeric self-healing adhesive. The unique role of adhesive functional groups in the formation of calcite crystals is confirmed by the absence of calcite crystals in the F1 mortars that had no STS-C additives.

This study demonstrated the synthesis of PMMA 2K self-healing additives via the miniemulsion technique. PMMA was found to be the most suitable shell material for the preservation and storage of Part A (resin + accelerator) and Part B (hardener) components. The advantages and disadvantages associated with their use as additives for concrete self-healing applications were then evaluated through four different mortar formulations. The mechanical resistance of the PMMA self-healing nanocapsules was not the leading cause of capsule breakage during mixing of developed formulations at early stages. The present study found that the mixing strategy and the mix design were two important factors in protecting nanocapsules from damages caused by the internal forces of concrete mixing and the impact forces of the aggregate, confirming the findings of previous studies. (Han and Xing 2017; Van Tittelboom and Belie 2013; Danish et al. 2020) An appropriate choice of mixing parameters (mixing blade, and agitation rate) and a suitable selection of admixtures have multiple benefits from preventing unwanted discharge of the healing agent from capsules during mixing (in addition to the shell wall

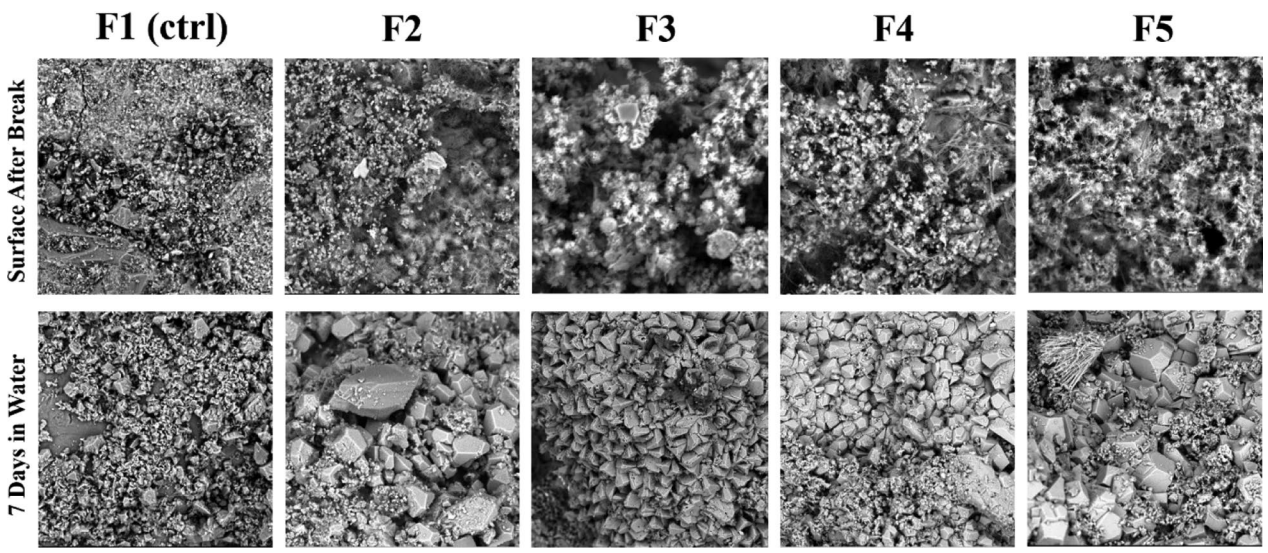

Fig. 9 SEM micrographs of the broken surfaces of self-healing mortar bars immediately after the three-point bending test (the first row), as well as the same surfaces after immersion in water for 7 days (the second row), the morphological changes in self-healing mortars and the sealing of voids is noticeable.

thickness), to reducing the concrete porosity, improving the workability, reducing the water intake, and finally evenly distributing Part A and Part B across the product matrix. They also can impact the compressive strength and fragility of self-healing concrete. The PMMA capsules had adequate adhesion to other components of the concrete matrix (including cement paste, aggregate), thus, cracking in concrete could trigger the capsule breakage. (Gruyaert et al. 2016) This 2K hybrid system has a more long-lasting healing effect than the MMA impregnation technique. Since, PMMA shell material can resist in concrete alkaline environment, consequently, can preserve the MMA monomers from the hydrolysis during the cement hydration and hardening stages. The F4 formulation was found to produce the strongest mortar sample (63 MPa compressive strength), with a good workability, acceptable distribution of Part A and Part B, and a lower w/c ratio. However, it was more brittle compared to the control mortar (F1).

The healing of cracks in the cementitious composites containing the developed 2K hybrid PMMA nanocapsules is expected to be a two-stage procedure: (a) the short-term healing occurs when healing agents (resin and hardener) are released into the microcrack lines, upon nanocapsules breakage. It takes a few seconds to minutes for the healing contents to react and produce polymeric chains to arrest the microcracks and restore the strength. (b) The long-term healing occurs when enough moisture penetrates the cement matrix. The carboxylate groups presented on the polymeric chains can catalyze the formation and growth of calcite crystals that gradually fill in excess voids and gaps. The later stage results in a dense and strong matrix in the long term.

In this study, approximately 1.3% (in parts weight) of the self-healing nanocapsules was used. The setting time of this adhesive system is quite short, but the amount of encapsulated resin and hardener within the nanocapsules is perhaps not enough to quickly fill all the emergent cracks. Increasing this amount to 5–10% parts weight in a concrete formulation, and the incorporation of appropriate custom-made dispersing agent, could increase the productivity of this system, though the formulation still needs to be adjusted (using other admixtures) to counteract the adverse effects of using a high amount of core–shell self-healing nanostructures and less amount of cement. Bigger capsules can increase the chance of releasing larger quantities of both self-healing materials at the crack site. (Hassan et al. 2016) Further research is needed to address these issues and refine this system prior to field studies. The partial replacement of cement with a self-healing additive, in the long term, can also benefit the global efforts for CO_2 emission reduction (Ghosh and Mandal 2018; UN 2015).

There are also numerous causes of cracking in concrete, and the initial laboratory results indicated the ability of this system to deal with controlled stress-induced cracks. Further investigation is required to address a range of structural damages, and to evaluate the robustness, effectiveness, and appropriateness of this system for different applications and outside laboratory settings. Simultaneous incorporation of self-healing nanocapsules into concrete in a larger scale production setting will also be challenging, as high-shear mixing can rupture numerous self-healing nanocapsules prior to the concrete hardening. Nor is the procedure for adding the two parts of self-healing agents (by separately preparing each part in the water phase) a desirable working procedure by the field operators. Further process optimization is therefore required to address the above-mentioned issues and facilitate the real-world implementation of this 2K self-healing system.

4 Conclusion

Core–shell nanocapsules composed of MMA + DMA core (resin and accelerator, Part A) and BPO core (hardener, Part B) encapsulated by PMMA and produced by the miniemulsion technique were shown to be an effective strategy for the controlled release of self-healing agents under induced stress conditions in cementitious materials. The step-by-step approach employed in the design of nanocapsules and the optimization of formulation and mixing procedure for the effective incorporation of these self-healing nanocapsules leads to the following key findings:

- The encapsulation of self-healing agents in PMMA was the only successful procedure, among three synthetic procedures employed, capable of generating stable nanocapsules with regular morphology, spherical surface, without aggregation, and mean diameters around 400 ± 100 nm (Part A) and 900 nm ± 100 nm (Part B).
- Consistent with previous findings, the results of this study indicated that the ultrasonication duration had a linear correlation with the nanocapsule diameter and the shell wall thickness. Nevertheless, it was very difficult to detect very small size nanocapsules (< 500 nm) embedded in mortar matrix using available SEM equipment.
- The optimum mix ratio of Part A:Part B was determined to be 1:0.3 (by mass) at 23 °C and relative humidity above 50%. The curing mechanism did not require moisture or open air and was completed in a few minutes.
- The mixing strategy (using a ribbon blade and a mixing speed of < 200 rpm) and the mix design

(addition of chemical admixtures) were found to have major impacts on the survival rate of nanocapsules in hardened mortar matrix.

- The addition of D-191 and D-192 dispersing agents facilitated the uniform distribution of healing components across the mortar matrix; however, this resulted in an increase in porosity and drying shrinkage and a decrease in the overall strength of the mortar. Nevertheless, the addition of copolymer binders to some extent counteracted the negative impacts of the addition of the dispersing agents.
- Although the addition of admixtures made mortar samples more brittle, the presence of superplasticizers and anti-shrinkage admixtures in developed formulation improved workability, reduced drying shrinkage, and the w/c ratio, and increased compressive strength.
- Developed self-healing nanostructures were correctly broken under induced stress and arrested the formed microcracks (< 10 μm). The healing of samples was found to be a two-stage procedure. The healing continued in the presence of sufficient moisture and calcite crystals filled in the empty voids in all samples.

The developed 2K PMMA self-healing system is, thus, expected to improve the durability of concrete products in long term.

Acknowledgments
We acknowledge the use of the Structural Research and Testing laboratory facilities at Western Sydney University, as well as facilities at the Centre for Nanoscale BioPhotonics, the Microscopy Unit and the GeoAnalytical laboratories at Macquarie University. Prof. Bijan Samali from Western Sydney University, Dr. Tom Lawson, Dr. Paritosh Giri, Dr. Timothy D. Murphy, Dr. Chao Shen, Mr. Vahik Avakian and Mr. Mark Tran from Macquarie University are acknowledged for their technical support. We thank Arezoo Razavi from ResChem Technologies, Denzil D'Mello, and Bruno D'Souza from BASF, and Dennis Keane from Wacker Chemicals for providing some of the samples and their technical support.

Author's information
Dr. ST: Faculty of Science and Engineering and Centre for Nanoscale BioPhotonics, Macquarie University, Room 207, 12 Wally's Walk, NSW 2109, Australia NSW 2109, Australia. Dr. ST is a Macquarie University Research Fellow (MQRF) and a member of Global Young Academy (GYA) with a PhD in Advanced Manufacturing and Mechanical Engineering. She is an expert on materials chemistry, nanotechnology, polymers, complex materials synthesis, and plasma polymerization. She has worked in both industrial R&D and academic roles always with an emphasis on developing and commercializing new products and technologies for diversified areas ranging from automotive through biomedical to construction materials, both in Australia and overseas. Her research interests are materials science and engineering, structural health monitoring, smart concrete (self-healing and self-sensing), nanotechnology, advanced manufacturing, adhesives, sealants and thin film coatings. E-mail: shima.taheri@mq.edu.au. P: + 61 2 9850 4725. Professor SMC: Faculty of Science and Engineering, Macquarie University, Room 131, 12 Wally's Walk, NSW 2109, Australia and Room 131, 50 Waterloo Road, Macquarie Park, NSW 2113, Australia. E-mail: simon.clark@mq.edu.au. P: + 61 2 9850 8166.

Authors' contributions
ST conceived the presented idea, designed and performed the experiments and wrote the manuscript. SMC helped supervise the project. Both authors read and approved the final manuscript.

Funding
This work is supported by a Macquarie University Research Fellowship (MQRF2018). The Centre for Nanoscale BioPhotonics (CNBP) at Macquarie University kindly provided laboratory access and some laboratory consumables.

Availability of data and materials
Some data generated or used during the study are proprietary or confidential in nature and may only be provided with restrictions.

Competing interests
The authors declare that they have no competing interests.

Author details
[1] Faculty of Science and Engineering and Centre for Nanoscale BioPhotonics, Macquarie University, North Ryde, NSW 2109, Australia. [2] Faculty of Science and Engineering and SmartCrete CRC, Macquarie University, North Ryde, NSW 2109, Australia.

Received: 9 June 2020 Accepted: 12 November 2020
Published online: 25 January 2021

References

ABS. (2018). *Construction Activity*. Australia: Australian Bureau of Statistic.
Ahangaran, F., Navarchian, A. H., & Picchioni, F. (2019). Material encapsulation in poly(methyl methacrylate) shell: a review. *Journal of Applied Polymer Science, 136,* 48039.
Alghamri, R., Kanellopoulos, A., & Al-Tabbaa, A. (2016). Impregnation and encapsulation of lightweight aggregates for self-healing concrete. *Construction and Building Materials, 124,* 910–921.
Araújo, M., Chatrabhuti, S., Gurdebeke, S., Alderete, N., Van Tittelboom, K., Raquez, J.-M., et al. (2018). Poly(Methyl Methacrylate) capsules as an alternative to the proof-of-concept" glass capsules used in self-healing concrete. *Cement and Concrete Composites, 89,* 260–271.
ASTM. (2018a). *C39/C39m-18, Standard Test Method for Compressive Strength of Cylindrical Concrete Specimens*. West Conshohocken, PA: ASTM International.
ASTM. (2018b). *C78/C78m-18 Standard Test Method for Flexural Strength of Concrete (Using Simple Beam With Third-Point Loading)*. West Conshohocken, Pa: ASTM International.
BCI_Economic. (2018). *Australian Construction Market Outlook Report 2018/2019*. Sydney: Bci Australia Pty Ltd.
Beglarigale, A., Seki, Y., Demir, N. Y., & Yazıcı, H. (2018). Sodium silicate/polyurethane microcapsules used for self-healing in cementitious materials: monomer optimization, characterization, and fracture behavior. *Construction and Building Materials, 162,* 57–64.
Camões, A., Aguiar, J.L.B., Jalali, S. (2005). Estimating compressive strength of concrete by mortar testing. In *Proceedings of INCOS 05 International Conference on Concrete for Structures* (pp 121–127). Coimbra, 7–8 July 2005, FCTUC, University of Coimbra, Coimbra.
Choi, H., Choi, H., Inoue, M., & Sengoku, R. (2017). Control of the polymorphism of calcium carbonate produced by self-healing in the cracked part of cementitious materials. *Applied Sciences, 7,* 546.
Danish, A., Mosaberpanah, M. A., & Usama Salim, M. (2020). Past and present techniques of self-healing in cementitious materials: a critical review on efficiency of implemented treatments. *Journal of Materials Research and Technology*. https://doi.org/10.1016/j.jmrt.2020.04.053.
De Belie, N., Gruyaert, E., Al-Tabbaa, A., Antonaci, P., Baera, C., Bajare, D., et al. (2018). A review of self-healing concrete for damage management of structures. *Advanced Materials Interfaces, 5,* 1800074.
De Larrard, F., & Belloc, A. (1997). The influence of aggregate on the compressive strength of normal and high-strength concrete. *Materials Journal, 94,* 417–426.

De Rooij, M., Van Tittelboom, K., De Belie, N., & Schlangen, E. (2011). *Self-Healing Phenomena in Cement-Based Materials: Draft of State-of-the-Art Report of Rilem Technical Committee*. Dorchert, The Netherlands: Springer.

Dry, C. M. (2000). Three designs for the internal release of sealants, adhesives, and waterproofing chemicals into concrete to reduce permeability. *Cement and Concrete Research, 30,* 1969–1977.

Dry, C., & Mcmillan, W. (1996). Three-part methylmethacrylate adhesive system as an internal delivery system for smart responsive concrete. *Smart Materials and Structures, 5,* 297–300.

Falini, G., Manara, S., Fermani, S., Roveri, N., Goisis, M., Manganelli, G., & Cassar, L. (2007). Polymeric admixtures effects on calcium carbonate crystallization: relevance to cement industries and biomineralization. *CrystEngComm, 9,* 1162–1170.

Feuser, P. E., Bubniak, L. D. S., Bodack, C. D. N., Valério, A., Silva, M. C. D. S., Ricci-Júnior, E., et al. (2016). In vitro cytotoxicity of poly(methyl methacrylate) nanoparticles and nanocapsules obtained by miniemulsion polymerization for drug delivery application. *Journal of Nanoscience and Nanotechnology, 16,* 7669–7676.

Frosch, R. J., & Jeffrey, S. (2007). *Causes, Evaluation, and Repair of Cracks in Concrete Structures*. American Concrete Institute: Farmington Hills.

Ghosh, A., & Mandal, A. (2018). Cement industry and strategies for mitigating carbon emissions. *International Research Journal of Advanced Engineering and Science, 3,* 175–178.

Gruyaert, E., Van Tittelboom, K., Sucaet, J., Anrijs, J., Van Vlierberghe, S., Dubruel, P., et al. (2016). Capsules with evolving brittleness to resist the preparation of self-healing concrete. *Materiales De Construcción, 66,* 092.

Gupta, S., Pang, S. D., & Kua, H. W. (2017). Autonomous healing in concrete by bio-based healing agents—A review. *Construction And Building Materials, 146,* 419–428.

Han, N.-X., & Xing, F. (2017). A comprehensive review of the study and development of microcapsule based self-resilience systems for concrete structures at Shenzhen university. *Materials, 10,* 2.

Hassan, M. M., Milla, J., Rupnow, T., Al-Ansari, M., & Daly, W. H. (2016). Microencapsulation of calcium nitrate for concrete applications. *Transportation Research Record, 2577,* 8–16.

Hilloulin, B., Van Tittelboom, K., Gruyaert, E., De Belie, N., & Loukili, A. (2015). Design of polymeric capsules for self-healing concrete. *Cement And Concrete Composites, 55,* 298–307.

Iqbal, K., & Sun, D. (2018). Synthesis of nanoencapsulated Glauber's salt using pmma shell and its application on cotton for thermoregulating effect. *Cellulose, 25,* 2103–2113.

Khan, N. I., Halder, S., & Goyat, M. S. (2016). Effect of epoxy resin and hardener containing microcapsules on healing efficiency of epoxy adhesive based metal joints. *Materials Chemistry And Physics, 171,* 267–275.

Landfester, K. (2001). the generation of nanoparticles in miniemulsions. *Advanced Materials, 13,* 765–768.

Landfester, K. (2009). Miniemulsion polymerization and the structure of polymer and hybrid nanoparticles. *Angewandte Chemie International Edition, 48,* 4488–4507.

Musyanovych, A., & Landfester, K. (2014). Polymer micro-and nanocapsules as biological carriers with multifunctional properties. *Macromolecular Bioscience, 14,* 458–477.

Pacheco-Torgal, F., Melchers, R., De Belie, N., Shi, X., Van Tittelboom, K., & Perez, A. S. (2017). *Eco-Efficient Repair And Rehabilitation Of Concrete Infrastructures*. Cambridge: Woodhead Publishing.

Rubio-Hernández, F. J., Velázquez-Navarro, J. F., & Ordóñez-Belloc, L. M. (2013). Rheology of concrete: a study case based upon the use of the concrete equivalent mortar. *Materials and Structures, 46,* 587–605.

Sarı, A., Alkan, C., & Bilgin, C. (2014). Micro/nano encapsulation of some paraffin eutectic mixtures with poly(methyl methacrylate) shell: preparation, characterization and latent heat thermal energy storage properties. *Applied Energy, 136,* 217–227.

Schindelin, J., Arganda-Carreras, I., Frise, E., Kaynig, V., Longair, M., Pietzsch, T., et al. (2012). Fiji: an open-source platform for biological-image analysis. *Nature Methods, 9,* 676–682.

Short, N. R. (2007). Degradation Of Polymer-Cement Composites (Chap. 10). *In:* Page, C. L. & Page, M. M. (Eds.) *Durability Of Concrete And Cement Composites.* Elsevier.

Souradeep, G., & Kua, H. W. (2016). Encapsulation technology and techniques in self-healing concrete. *Journal of Materials in Civil Engineering, 28,* 04016165.

Taheri, S. (2019). A review on five key sensors for monitoring of concrete structures. *Construction and Building Materials, 204,* 492–509.

Taheri, S., Baier, G., Majewski, P., Barton, M., Förch, R., Landfester, K., & Vasilev, K. (2014a). Synthesis and antibacterial properties of a hybrid of silver-potato starch nanocapsules by miniemulsion/polyaddition polymerization. *Journal of Materials Chemistry B, 2,* 1838–1845.

Taheri, S., Baier, G., Majewski, P., Barton, M., Förch, R., Landfester, K., & Vasilev, K. (2014b). Synthesis and surface immobilization of antibacterial hybrid silver-poly (L-lactide) nanoparticles. *Nanotechnology, 25,* 305102.

Talaiekhozan, A., Keyvanfar, A., Shafaghat, A., Andalib, R., Majid, M. A., Fulazzaky, M. A., et al. (2014). A review of self-healing concrete research development. *Journal of Environmental Treatment Techniques, 2,* 1–11.

Tommasini, F. J., Ferreira, L. D. C., Tienne, L. G. P., Aguiar, V. D. O., Silva, M. H. P. D., Rocha, L. F. D. M., & Marques, M. D. F. V. (2018). Poly (Methyl Methacrylate)-sic nanocomposites prepared through in situ polymerization. In M. D. Hager, S. van der Zwaag, & U. S. Schubert (Eds.), *Materials Research* (pp. 345–385). Cham: Springer.

Tommasini, F. J., Ferreira, L. D. C., Tienne, L. G. P., Aguiar, V. D. O., Silva, M. H. P. D., Rocha, L. F. D. M., & Marques, M. D. F. V. (2018). Poly (Methyl Methacrylate)-Sic Nanocomposites Prepared Through In Situ Polymerization. *Materials Research*. https://doi.org/10.1590/1980-5373-mr-2018-0086.

UN. (2015). *Sustainable Development Goals: 17 Goals To Transform Our World*. Newyork, NY: United Nations.

Vaishya, R., Chauhan, M., & Vaish, A. (2013). Bone cement. *Journal of Clinical Orthopaedics and Trauma, 4,* 157–163.

Van Tittelboom, K., Adesanya, K., Dubruel, P., Van Puyvelde, P., & De Belie, N. (2011). Methyl Methacrylate as a healing agent for self-healing cementitious materials. *Smart Materials and Structures, 20,* 125016.

Van Tittelboom, K., & De Belie, N. (2013). Self-healing in cementitious materials—a review. *Materials, 6,* 2182–2217.

White, S. R., Sottos, N. R., Geubelle, P. H., Moore, J. S., Kessler, M. R., Sriram, S., et al. (2001). Autonomic healing of polymer composites. *Nature, 409,* 794.

Wool, R. P. (2008). Self-healing materials: a review. *Soft Matter, 4,* 400–418.

Yeon, K.-S., Jin, N. J., & Yeon, J. H. (2018). Effect of methyl methacrylate monomer on properties of unsaturated polyester resin-based polymer concrete. In M. M. Reda Taha (Ed.), *International Congress on Polymers in Concrete* (pp. 165–171). Cham: Springer.

Zhao, Y., Fickert, J., Landfester, K., & Crespy, D. (2012). Encapsulation of self-healing agents in polymer nanocapsules. *Small (Weinheim an der Bergstrasse, Germany), 8,* 2954–2958.

Zydowicz, N., Nzimba-Ganyanad, E., & Zydowicz, N. (2002). Pmma microcapsules containing water-soluble dyes obtained by double emulsion/solvent evaporation technique. *Polymer Bulletin, 47,* 457–463.

Publisher's Note